Volume XXIX 2026
MBNA Publishing House Constanta 2026



Scientific Bulletin of Naval Academy

SBNA PAPER • OPEN ACCESS

Structural integrity and ultimate strength of tubular joints in naval architecture

To cite this article: Birsan Dan-Catalin, Scientific Bulletin of Naval Academy, Vol. XXIX 2026, pg. 223-232.

Submitted: 23.04.2026
Revised: 25.08.2026
Accepted: 22.09.2026

Available online at www.anmb.ro

ISSN: 2392-8956; ISSN-L: 1454-864X

doi: 10.21279/1454-864X-26-I1-022
SBNA© 2026. This work is licensed under the CC BY-NC-SA 4.0 License

Structural integrity and ultimate strength of tubular joints in naval architecture

Birsan Dan-Catalin[1]*

[1]"Dunarea de Jos" University, Faculty of Engineering, Manufacturing Engineering Department, dbirsan@ugal.ro

***dbirsan@ugal.ro**

Abstract. Tubular joints are fundamental components in the design of offshore platforms, naval vessels, and marine superstructures, offering high strength-to-weight ratios and favourable hydrodynamic behaviour. Because their welded intersections concentrate multiaxial loads, they are among the most vulnerable regions of any marine tubular framework. This paper presents a static, linear-elastic finite element assessment of the punching-shear integrity of welded tubular joints in naval architecture, formulated as a general applied-naval-architecture methodology and illustrated through the representative case of an offshore helideck supporting structure. Two critically loaded connections, denoted J1 and J2, are evaluated under the combined action of dynamic landing impact, sympathetic-response amplification, superimposed deck load, lateral and dead loads, and 100-year return-period wind, applied in accordance with CAP 437 and ABS rules. Load-bearing capacity is quantified using the API RP 2A-WSD parametric framework, based on the dimensionless strength and chord-load factors and the joint interaction ratio (IR). The interaction ratios remain below unity for all load combinations, reaching 0.29 for joint J1, governed by in-plane bending, and 0.34 for joint J2, governed by out-of-plane bending under eccentric landing, thereby confirming adequate margins against chord-face plastification and punching shear. A parametric study shows that joint capacity is most sensitive to the brace-to-chord diameter ratio β, while the chord slenderness ratio γ acts as a secondary factor. The extension of this linear-elastic assessment to non-linear elasto-plastic finite element modelling and scaled experimental validation is identified as the principal direction for future work.

Keywords: tubular joints; finite element analysis (FEA); naval architecture; structural integrity.

1. Introduction

This chapter introduces the problem of punching shear in tubular helideck structures, outlining its practical significance and reviewing the relevant literature in the field.

Tubular members, particularly Circular Hollow Sections (CHS), are extensively utilized in the construction of offshore platforms, naval vessels, and marine superstructures. Their widespread adoption is primarily driven by their excellent omnidirectional buckling resistance, high strength-to-weight ratio, and favorable hydrodynamic profile, which significantly minimizes drag forces from wind and wave actions. However, the welded intersections of these members, commonly referred to as tubular joints, represent the most critical and vulnerable components within the structural framework. Due to abrupt geometric transitions, these joints are subjected to severe local stress concentrations and multiaxial environmental loading, rendering them highly susceptible to localized yielding and ultimate failure (Wardenier, 1982; Marshall, 1992).

The ultimate strength and predominant failure mechanisms of these connections—such as chord face plastification, punching shear, and brace local buckling—are fundamentally governed by their non-dimensional geometric parameters. Specifically, the structural response is dictated by the brace-to-chord

diameter ratio (β), the chord radius-to-thickness ratio (γ), and the brace-to-chord wall thickness ratio (τ) (Kurobane et al., 1984). Understanding how these parameters interact under extreme loading conditions is essential for preventing catastrophic structural collapse.

Currently, the design and safety assessment of marine tubular structures rely heavily on established industry guidelines, most notably the American Petroleum Institute standards (API, 2014) and Det Norske Veritas offshore codes (DNV, 2015). These codes provide parametric equations for calculating the load-bearing capacity of standard joint configurations, such as T, Y, K, and X joints. These formulations are predominantly empirical, having been derived and calibrated over decades using extensive international databases of scaled experimental tests (Makino et al., 1996). While these standards ensure a robust baseline for safe design, they frequently rely on simplified assumptions. Consequently, they may yield overly conservative or, conversely, un-conservative estimations when applied to joints subjected to complex, combined loading scenarios or when utilizing modern high-strength steels.

To overcome the high financial costs and physical limitations associated with large-scale destructive testing, non-linear Finite Element Analysis (FEA) has become an indispensable tool in modern naval architecture. Advanced numerical modeling allows for an in-depth investigation of elasto-plastic deformation, localized stress distributions, and the complex influence of boundary conditions on chord load effects (Lee, 1999; van der Vegte et al., 2001). Furthermore, applying precise deformation limits—such as Yura's deformation limit—is crucial for accurately defining the ultimate strength criteria within virtual simulations, ensuring that the numerical models closely replicate physical joint yielding (Lu et al., 1994; Choo et al., 2003).

In this context, the present study addresses the structural integrity and punching-shear behaviour of welded tubular joints in naval architecture by means of a static, linear-elastic finite element assessment. Rather than being confined to a single design, the work is conceived as a general study in applied naval architecture: it sets out a methodology for evaluating the load-bearing capacity of tubular connections under combined loading, and then demonstrates that methodology on a representative and particularly demanding example, namely the tubular supporting structure of an offshore naval heliport. This case study allows the interaction of combined axial forces and biaxial bending to be examined under a realistic multiaxial load envelope, while the applicability of the current API RP 2A-WSD design provisions is examined against the computed joint response. Non-linear elasto-plastic modelling and scaled experimental validation, although beyond the scope of the present linear-elastic study, are identified as the principal directions for subsequent research.

2. Theoretical framework

This chapter presents the theoretical background of the punching shear phenomenon according to (API, 2014), including the fundamental principles and governing equations used in its analysis.

Connections at the ends of tension and compression members must satisfy a minimum capacity requirement: they shall develop no less than 50% of the effective strength of the connected member. The effective strength is defined as the buckling resistance for members under compressive or combined loading, and as the yield axial capacity for members governed primarily by tension. Welds at tubular member ends must develop the lesser of: (1) the yield strength of the branch member cross-section, or (2) the chord capacity as governed by the basic capacity equations.

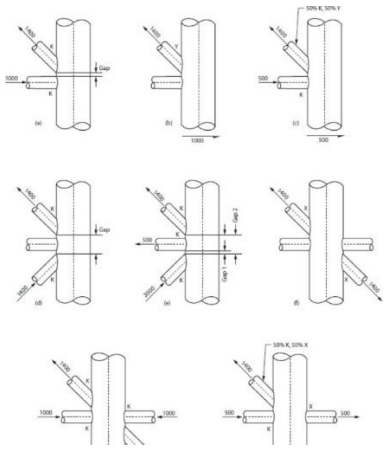


Figure 1. Examples of Joint Classification Illustrating K, X, and Y Load Components

Simple joints are defined as connections in which principal braces do not overlap and in which no reinforcing elements, gussets, diaphragms, grout infill, or ring stiffeners, are present. The capacity formulations described in this section are applicable within the following validity range: diameter ratio $0.2 \leq \beta \geq 1.0$; chord slenderness ratio $10 \leq \gamma \geq 50$; brace inclination $30° \leq \theta \geq 90°$; chord yield stress $F_y \leq 500$ MPa; and, for K-joints, normalized gap $g/D > -0.6$. The geometric parameters defining a simple tubular joint are illustrated in Figure 2.

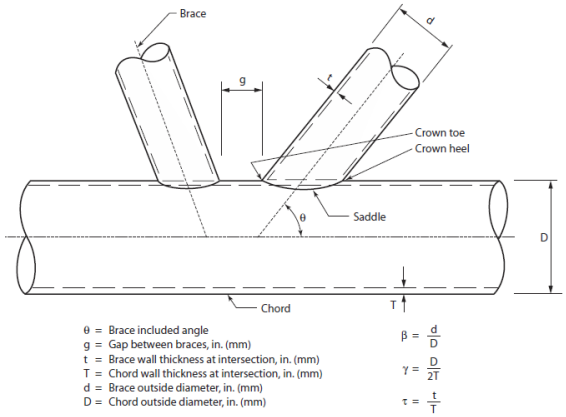


Figure 2. Terminology and Geometric Parameters for Simple Tubular Joints

The allowable axial capacity P_a and the allowable bending moment capacity M_a for a simple tubular joint are given by Eq. 1 and 2, respectively, which express capacity as a function of chord material properties, chord wall geometry, joint classification factors, and brace inclination:

$$P_a = Q_u \cdot Q_f \frac{F_{yc} \cdot T^2}{FS \cdot sin\theta} \quad (1)$$

$$M_a = Q_u \cdot Q_f \frac{F_{yc} \cdot T^2 \cdot d}{FS \cdot sin\theta} \quad (2)$$

where:

P_a = allowable capacity for brace axial load,

M_a = allowable capacity for brace bending moment,

F_{yc} = the yield stress of the chord member at the joint (or 0.8 of the tensile strength, if less), MPa,

FS = safety factor = 1.60.

The dimensionless strength factor Q_u captures the influence of joint geometry (primarily the diameter ratio β and chord slenderness γ) and the mode of brace loading on the localised plastification capacity

of the chord wall. Its values for the three joint classifications and four loading modes are tabulated in Table 1.

Table 1. Values for Q_u

Joint Classification	Brace Load			
	Axial Tension	Axial Compression	In-Plane Bending	Out-of-Plane Bending
K	$(16+1.2\cdot\gamma)\cdot\beta^{1.2}\cdot Q_g$ but $\leq 40\cdot\beta^{1.2}\cdot Q_g$			
T/Y	$30\cdot\beta$	$2.8+(20+0.8\cdot\gamma)\cdot\beta^{1.6}$ but $\leq 2.8+36\cdot\beta^{1.6}$	$(5+0.7\cdot\gamma)\cdot\beta^{1.2}$	$2.5+(4.5+0.2\cdot\gamma)\cdot\beta^{2.6}$
X	$23\cdot\beta$ for $\beta \leq 0.9$ $20.7+(\beta-0.9)\cdot(17\cdot\gamma-220)$ for $\beta > 0.9$	$[2.8+(12+0.1\cdot\gamma)\cdot\beta]\cdot Q_\beta$		

Q_β is a geometric factor defined by:

$$Q_\beta = \begin{cases} \frac{0.3}{\beta\cdot(1-0.833\cdot\beta)} & for\ \beta > 0.6 \\ 1 & for\ \beta \leq 0.6 \end{cases} \quad (3)$$

Q_g is the gap factor defined by:

$$Q_g = \begin{cases} 1+0.2\cdot[1-2.8\cdot g/D]^3 & for\ \frac{g}{D} \geq 0.05\ but \geq 1.0 \\ 0.13+0.65\cdot\phi\cdot\gamma^{0.5} & for\ \frac{g}{D} \leq -0.05\ where\ \phi = t\cdot F_{yb}/(TF_y) \end{cases} \quad (4)$$

F_{yb} = yield stress of brace or brace stub if present (or 0.8 times the tensile strength if less), MPa.

Table 2. Values for C_1, C_2, C_3

Joint Type	C_1	C_2	C_3
K joints under brace axial loading	0.2	0.2	0.3
T/Y joints under brace axial loading	0.3	0	0.8
X joints under brace axial loading			
$\beta \leq 0.9$	0.2	0	0.5
$\beta = 1.0$	-0.2	0	0.2
All joints under brace moment loading	0.2	0	0.4

The joint interaction ratio, IR, for axial loads and/or bending moments in the brace should be calculated using the following expression:

$$IR = \left|\frac{P}{P_a}\right| + \left(\frac{M}{M_a}\right)^2_{ipb} + \left|\frac{M}{M_a}\right|_{opb} \leq 1.0 \quad (5)$$

3. Case Study and Calculation Methodology

This chapter describes the assessment methodology and its application to a representative real-world example of a tubular naval structure: the supporting framework of an offshore helideck to be installed on a drilling vessel. The helideck is designed for a SIKORSKY S92A helicopter, which is used here solely to define the governing landing and inertia loads; the focus of the study remains the structural behaviour of the tubular joints that carry them.

The analysis is carried out by means of a finite element model and constitutes a static, linear-elastic assessment based on the calculation of combined loads.

Steel used in the structural design is High Tensile steel Grade HT36 with a minimum yield point of 355 N/mm^2 for helideck structure and supporting reinforcements, API 5L Grade X52 for pipe and steel Grade A with a minimum yield point of 235 N/mm^2 for hull structure.

3.1. Loading cases and loads

The loading cases have been considered according to:

- Offshore Helicopter Landing Areas - Guidance on Standards-CAP 437 (CAA, 2026, Chapter 3 Paragraph 4);
- ABS-Rules for Building and Classing-Mobile Offshore Drilling Units-Part 3-Hull Construction and Equipment (ABS, 2025, Part 3 Ch. 2 Sect. 2).

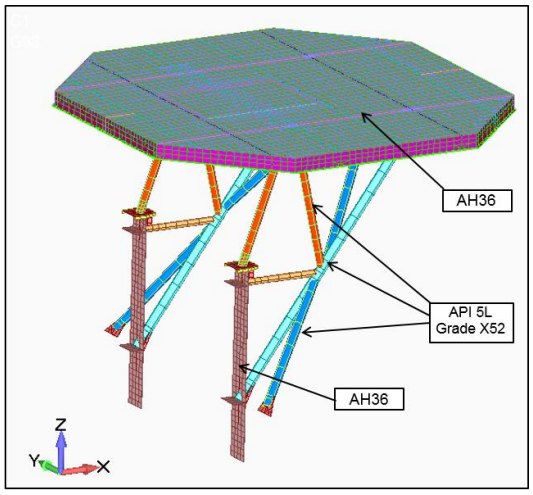


Figure 3. Height Tensile Strength Steel for Helideck Structure

According to (CAA, 2026) the following must be taken into account:

Dynamic load due to impact landing

$F_z = 1.5 \cdot MTOM = 1.5 \cdot 12565 \text{ x } 9.81 = 184.894$ kN

A pair of two forces Fz was applied on the deck; the distance between the forces (wheels) is 3.18 m.

Sympathetic response of landing platform

The dynamic load (see above) was increased by a minimum structure response factor of 1.3. Therefore:

$1.3 \cdot F_z = 1.3 \cdot 184.894 = 240.362$ kN

Overall superimposed load on the landing platform

To allow for any appendages that may be present on the deck surface (e.g. helideck net, "H" and circle lighting etc.) in addition to wheel loads, an allowance of 0.5 kN/m2 was added over the whole area of the helideck.

ps = 0.5 kN/m^2.

Lateral load on landing platform supports

$F_h = 0.5 \cdot 0.5 \cdot MTOM = 0.5 \cdot 0.5 \cdot 9.81 \cdot 12.565 = 30.816$ kN,

applied in the horizontal plane on each wheel in two directions x, y, separately.

Dead load of structural members

This is the normal gravity load on the element being considered.

The weights of the walkways, stairs hand rails, helideck perimeter light, fire fight system pipes were considered as separately loads, as values 13.5 tons which acting on the perimeter of the helideck.

Wind forces for DOC

The 100-year return period wind actions were applied in the direction which together with the imposed lateral loading, will produce the most severe loadings on structure.

The calculation of wind pressure, P, the following equation is to be used and the vertical height is to be subdivided approximately.

$P = f \cdot V_k^2 \cdot C_h \cdot C_s$, where:

F = 0.611; V_k – wind velocity in m/s; C_h – height coefficient; C_s – shape coefficient.

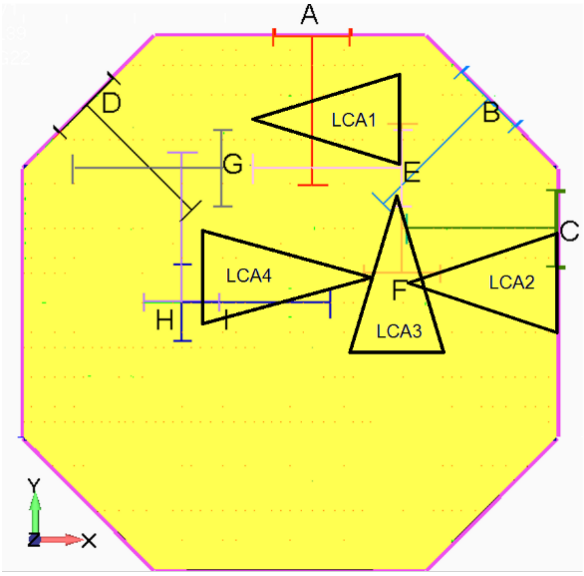


Figure 4. Helicopter landing positions

4. Results and Discussion

This chapter presents and discusses the results obtained from the analysis, highlighting their significance in relation to the studied phenomenon. The joints considered for the analysis of the punching shear phenomenon are denoted by J1 and J2 and can be seen in Figure 5.

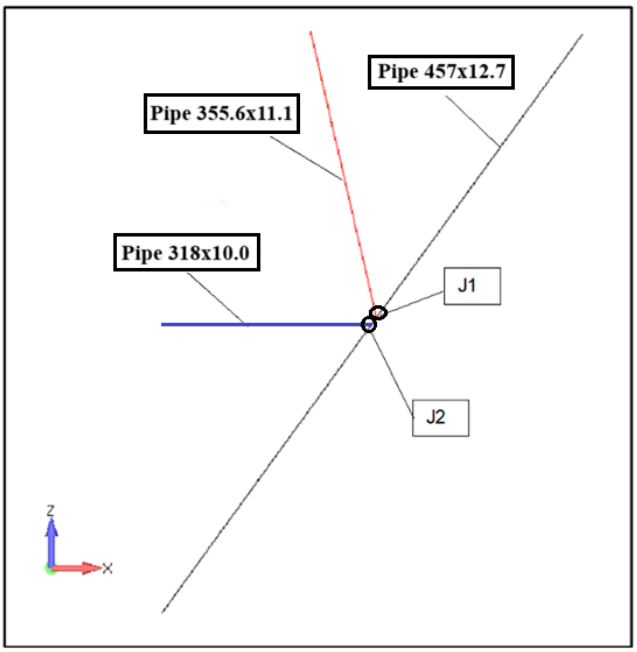


Figure 5. The tubular joints considered for punching shear assessment

The envelopes of axial forces and in- and out-of-plane moments can be observed in Figure 6.

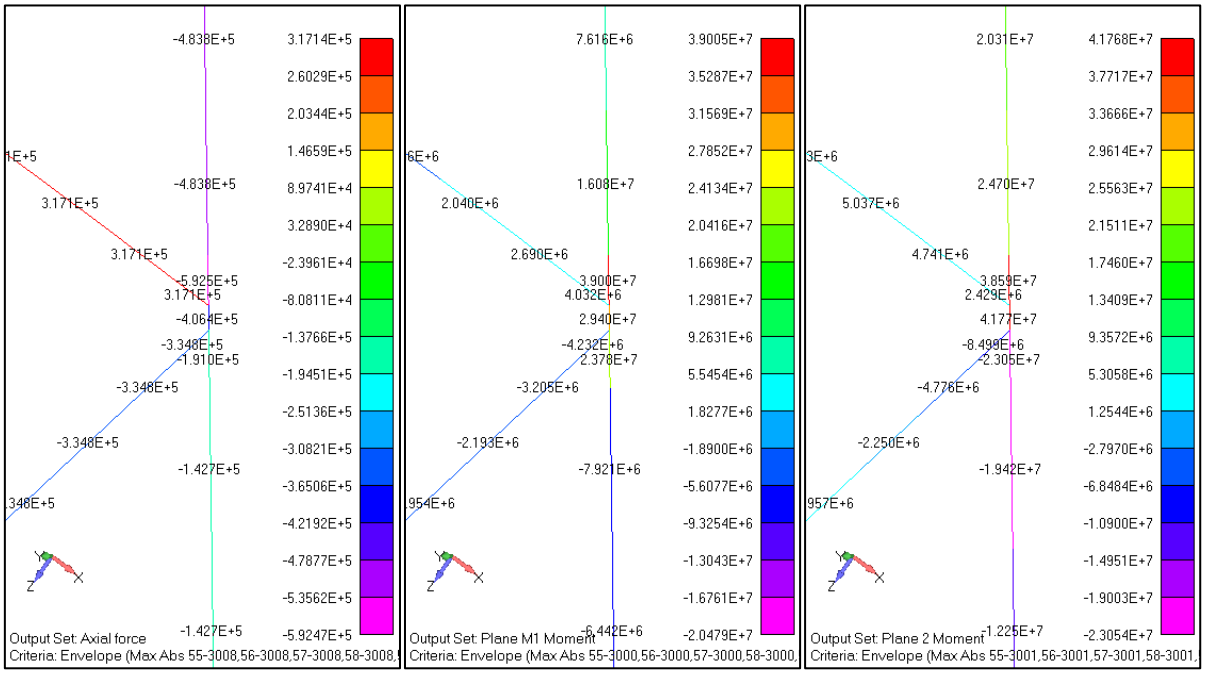


Figure 6. Envelopes of axial forces, in-plane and out-of-plane moments for tubular joints J1 and J2

The punching shear assessment of joints J1 and J2, the most critically loaded connections within the helideck structure, confirmed that both are subjected to combined axial forces and biaxial bending moments. The governing load envelope arises from the simultaneous application of the dynamic landing impact, the amplified sympathetic response factor, and the 100-year wind action. J1 is predominantly loaded in compression, while J2 exhibits a mixed tension-compression regime depending on the helicopter landing position.

Interaction ratios (IR) per Eq. 5 remained below 1.0 for all load combinations. Joint J1 reached a peak IR of 0.29 under combined dynamic impact and transverse wind, with in-plane bending dominant; joint J2 recorded a peak IR of 0.34 under the eccentric landing scenario (Position 2), governed by out-of-plane bending. Both values confirm operation within the elastic range, with adequate margins against chord face plastification and punching shear failure.

A parametric study on β and γ showed that structural response is most sensitive to β: increasing it from 0.5 to 0.7 reduced axial capacity P_a by 34% for T/Y loading modes, consistent with the Q_β formulation (Eq. 3). Reducing γ by increasing chord wall thickness T produced proportional capacity gains through the T^2 dependency in Eqs. 1 and 2.

Weld capacity checks confirmed that the fillet welds at both brace-to-chord intersections develop the required capacity, with throat dimensions sufficient for the governing combined stress state, and no punching-shear overstress was identified at either location. Taken together, these results illustrate a behaviour that is generic to welded tubular connections rather than specific to the present installation: the punching-shear demand is concentrated at the brace-chord interface and is governed by the combination of axial load and biaxial bending transmitted through the joint, so that the geometric parameters of the connection, more than the absolute magnitude of the applied loads, dictate the available margin. For the example considered, the HT36 primary framework and the API 5L Grade X52 pipe members provide this margin comfortably under the full CAP 437 load envelope.

		J1	J2	
Chord diameter	D =	**457.0**	**457.0**	[mm]
Brace diameter	d =	**355.6**	**318.0**	[mm]
Chord thickness	T =	**12.7**	**12.7**	[mm]
Brace thickness	t =	**11.1**	**10.0**	[mm]
Gap	g =	**140.0**	**140.0**	[mm]
Brace angle	Q =	**49.0**	**54.0**	[grd]
Joint type		K	K	
	t = t/T =	0.87	0.79	
	b = d/D =	0.78	0.70	
	g = D/2T =	17.99	17.99	
Yield stress	Fy =	**359**	**359**	[MPa]
The validity range		**OK**	**OK**	
Allowable capacity for brace axial load	Pa =	1.33E+06	1.10E+06	N
Allowable capacity for brace in plane bending moment	(Ma)ipb =	2.21E+08	1.63E+08	Nm
Allowable capacity for brace out of plane bending moment	(Ma)opb =	1.14E+08	8.10E+07	Nm
Safety factor	FS =	**1.6**	**1.6**	
Strength factor	Qu_a =	27.83	24.34	
	Qu_ipb =	13.02	11.39	
	Qu_opb =	6.72	5.65	
Gap factor	Qg =	1.00	1.00	
	Qf =	1.00	1.01	
C1, C2, C3 - coefficients depending on joint and load type	C1 =	**0.2**	**0.2**	
	C2 =	**0.2**	**0.2**	
	C3 =	**0.3**	**0.3**	
	A =	0.08	0.18	
Nominal axial load in the chord	Pc =	**-1.91E+05**	**5.93E+05**	[N]
Nominal bending in plane in the chord	Mipb =	**-2.31E+07**	**3.86E+07**	[Nmm]
Nominal bending out of plane in the chor	Mopb =	**2.38E+07**	**3.90E+07**	[Nmm]
Nominal bending resultant in the chord	Mc =sqrt(Mipb^2+Mopb^2)	3.31E+07	5.49E+07	[Nmm]
Chord area	S =	**1.77E+04**	**1.77E+04**	[mm2]
Yield axial capacity of the chord	Py=	6.36E+06	6.36E+06	[N]
Plastic section modulus of the chord	Wp=	**2.51E+06**	**2.51E+06**	[mm3]
Plastic moment capacity of the chord	Mp=	9.00E+08	9.00E+08	[Nmm]
Nominal axial load in the brace	P =	**-3.35E+05**	**3.17E+05**	[N]
Nominal bending in plane in the brace	(Ma)ipb =	**-8.50E+06**	**2.43E+06**	[Nmm]
Nominal bending out of plane in the brac	(Ma)opb =	**-4.23E+06**	**4.03E+06**	[Nmm]
Strength Check	IR =	0.29	0.34	
		OK	**OK**	

Figure 7. Punching shear results

5. Conclusions

This study investigated the structural integrity and ultimate strength of welded tubular joints J1 and J2 within a helideck supporting structure designed for offshore operations. A static elastic linear finite element assessment was conducted in compliance with CAP 437 (CAA, 2026) and ABS Rules for Mobile Offshore Drilling Units (ABS, 2025), incorporating dynamic landing impact loads, sympathetic response amplification, superimposed deck loads, lateral forces, dead loads, and 100-year return period wind actions. The punching shear capacity of both joints was evaluated using the API RP 2A-WSD parametric framework, applying the dimensionless strength factor Q_u, the chord load reduction factor Q_f, and the joint interaction ratio IR for combined axial and biaxial bending loading.

The principal conclusions drawn from the analysis are as follows. Both joints J1 and J2 satisfy the punching shear capacity requirements under all considered load combinations, with maximum interaction ratios of 0.29 and 0.34, respectively, confirming adequate safety margins. The governing failure mode for joint J1 under combined dynamic and wind loading is chord face plastification driven by in-plane bending, while joint J2 is more critically influenced by out-of-plane bending arising from eccentric helicopter landing positions. These findings highlight the importance of considering all prescribed landing positions defined in CAP 437 when assessing the structural integrity of offshore helideck tubular connections.

The parametric study confirmed that the brace-to-chord diameter ratio β is the most influential geometric parameter governing joint capacity, consistent with the established literature (Kurobane et al., 1984; Makino et al., 1996). Reducing β by increasing the chord diameter or decreasing the brace diameter provides the most effective means of improving punching shear resistance without significant weight penalty. The chord slenderness ratio γ was identified as a secondary but non-negligible parameter: thicker chord walls substantially increase capacity through the T^2 term in the capacity equations, and their adoption is particularly recommended for joints subjected to high out-of-plane bending demands in harsh marine environments.

The use of High Tensile steel Grade HT36 (Fy = 355 N/mm²) for the primary helideck structure and API 5L Grade X52 for the pipe members proved appropriate for the loading conditions considered. The higher yield strength of HT36 relative to standard Grade A steel (Fy = 235 N/mm²) provides a 51% increase in the theoretical chord capacity, contributing directly to the satisfactory interaction ratios recorded. However, designers should remain attentive to the API RP 2A-WSD upper limit of Fyc ≤ 500 MPa (or 0.8 × tensile strength if less) when applying these formulations to higher-strength steels, in order to avoid unconservative estimates of chord face plastification resistance.

Future research directions should focus on extending the current static elastic assessment to a non-linear elasto-plastic FEA framework in order to capture post-yield redistribution and to quantify the residual capacity beyond the elastic limit. The influence of weld geometry imperfections, corrosion-induced wall thinning, and fatigue crack initiation at the brace-chord intersection, all of which are prevalent degradation mechanisms in offshore marine environments, should be incorporated into a comprehensive structural integrity management strategy. Additionally, the application of Yura's deformation limit criterion within non-linear numerical models would allow more precise ultimate strength predictions, enabling the calibration of refined parametric equations that could supplement or improve upon the current API and DNV code provisions for complex combined loading scenarios involving high-strength steels.

Acknowledgements
Yes, I confirm that all individuals named in the acknowledgements have agreed to being included.

Author contributions: Conceptualization: B.D.C.; Methodology: B.D.C.; Investigation: B.D.C.; Writing original draft: B.D.C.; Writing review and editing: B.D.C.; Supervision: B.D.C.

Funding: this research received no external funding.

Conflict of interest: The Author declare no Conflict of interest.

References

1. Wardenier, J. (1982). Hollow Section Joints. Delft University Press.
2. Marshall, P. W. (1992). Design of Welded Tubular Connections: Basis and Use of AWS Code Provisions. Elsevier.
3. Kurobane, Y., Makino, Y.and Ochi, K. (1984). Ultimate resistance of unstiffened tubular joints. Journal of Structural Engineering, 110(2), 385-400.
4. Lee, M. M. K. (1999). Strength, stress and fracture analyses of offshore tubular joints using finite elements. Journal of Constructional Steel Research, 51(3), 251-270.
5. van der Vegte, G. J., Makino, Y. and Kurobane, Y. (2001). Influence of boundary conditions on chord load effects for CHS T-and X-joints. Journal of Constructional Steel Research, 57(8), 785-802.
6. Choo, Y. S., Qian, X. D., Liew, J. Y. R. and Wardenier, J. (2003). Static strength of thick-walled CHS X-joints: Part I. New approach in strength definition. Journal of Constructional Steel Research, 59(10), 1201-1228.

7. Lu, L. H., de Winkel, G. D., Yu, Y. and Wardenier, J. (1994). Deformation limit for the ultimate strength of hollow section joints. Tubular Structures VI, 341-347.
8. Makino, Y., Kurobane, Y., Ochi, K., van der Vegte, G. J. and Wilmshurst, S. R. (1996). Database of test and numerical analysis results for unstiffened tubular joints. IIW Doc. XV-E-96-220. International Institute of Welding.
9. API (American Petroleum Institute). (2014). API Recommended Practice 2A-WSD: Planning, Designing, and Constructing Fixed Offshore Platforms - Working Stress Design (22nd ed.). Washington, DC: API.
10. Cap437 Standards for Offshore Helicopter Landing Areas, Jan. 2026.
11. ABS- Rules for Building and Classing Mobile Offshore Drilling Units, July 2025.